

## OPTIMIZATION AND STORAGE OF WATER-IN-OIL EMULSION USING A SUPPLEMENTED AQUEOUS PHASE AND SUNFLOWER OIL

ADRIANA MICANQUER-CARLOSAMA<sup>1,\*</sup>,  
CORTÉS-RODRÍGUEZ, MISAEL<sup>2</sup>, SERNA-COCK, LILIANA<sup>3</sup>

<sup>1</sup>Facultad de Ciencias. Universidad Nacional de Colombia. Campus Medellín. Colombia

<sup>2</sup>Departamento de Ingeniería Agrícola y Alimentos, Facultad de Ciencias Agrarias.  
Universidad Nacional de Colombia. Campus Medellín. Colombia. Tel (+ 57-4) 4309065

<sup>3</sup>Departamento de Ingeniería, Facultad de Ingeniería y Administración. Universidad  
Nacional de Colombia. Campus Palmira. Colombia. Tel (+57-2) 2868888 Ext. 35720

\*Corresponding Author: armicanquerc@unal.edu.co

### Abstract

Emulsions are complex systems, thermodynamically unstable, and widely used across the food, pharmaceutical, and cosmetic industries. The objective of the research was to optimize the formulation and process for obtaining a water-in-oil (W/O) emulsion, using a supplemented aqueous phase (pineapple and sachinchi wastes, and mineral salts) and sunflower oil; and to evaluate its stability during short storage (3 days at 4°C). Response surface methodology (RSM) and a central compound design were used to define the optimal formulation and process. The independent variables: homogenization time (HT) (1-5 min), total hydrophile-lipophile balance ( $HLB_{total}$ ) (4.7-6.7), surfactants (Tween 80+Span 60) (0.1-0.5%), and oil (30-50%) and dependent variables: viscosity, zeta potential ( $\zeta$ ), cremated index, particle size, and the spectral absorbance stability index were considered. In general, the independent variables and their linear interactions affected the stability of the low viscosity emulsions. The optimal conditions were HT: 3.73 min,  $HLB_{total}$ : 6.53, surfactants: 0.47%, and oil: 39.6%. A stable emulsion was obtained as to consequence of the repulsive forces generated by the double electrical layer formed at the interface of the particles. The models are adequate to describe the behavior of the results found; since, the variables presented a random distribution of the residuals, which makes it possible to ensure that the data can be parameterized according to a normal distribution. Additionally, spherical, homogeneous, slightly flocculated, and small size drops were observed. During storage, the emulsion remained stable with a high negative electrical potential ( $\zeta$ : -41.40±1.90 mV). The use of agro-industrial waste in the formulation of emulsions favors the sustainability of production systems in the context of a circular economy.

Keywords: *Ananas comosus*, Colloidal system, electrostatic forces, *Plukenetia volubilis*, Van der Waals forces, viscosity.

## 1. Introduction

The food, pharmaceutical, chemical, and cosmetic industries frequently formulate products based on single emulsions (O/W, W/O) and double emulsions (W/O/W or O/W/O) [1, 2]. Consequently, there is a growing trend in demand for this of products in the world market [3, 4]. On the other hand, colloidal systems are thermodynamically unstable and complex (phenomena of creaming, sedimentation, flocculation, Ostwald ripening, and coalescence) [5-7]. The instability phenomena occur due to excess free energy at the interface of the dispersed drops; which are caused by different forces including: attractive or Van der Waals, repulsive or electrostatic, steric, hydrophilic, and hydrophobic [8, 9].

Multiple studies have highlighted the effect of attractive forces on emulsion stability based on drop sizes (nano or micro) [10, 11]. Those sizes depend on the operating conditions applied (homogenization speed, the gap of the rotor-stator system, recirculation or direct passage, pressure, and homogenization time, among others) [12-14]. Similarly, other research highlights the importance of repulsive forces, due to the generation of an electrical double layer around the particles. The double layer has a sufficiently low charge density to keep the particles dispersed and reduce their attraction [15]. Other factors associated with emulsion instability include the composition of the emulsions [16, 17]; formulation and process parameters (pH, ionic force, and temperature) [11, 18], and the presence of surfactants. The main function of surfactants is to lower surface tension, as they have an affinity for the polar or non-polar parts of the emulsion components [14]. The use of total surfactant (Span and Tween) makes it possible to modify the hydrophilic-lipophilic balance (HLB) and consequently to enhance its affinity with hydrophilic or lipophilic molecules [6]. Span and Tween are non-ionic surfactants, stable, non-reactive with ionic ingredients, and safe; therefore, they are widely used in the formulation of colloidal systems [10, 19].

On the other hand, the constant generation of agro-industrial waste worldwide causes an accumulation of organic materials that are difficult to handle, resulting in drastic effects on the environment [20, 21]. For example, waste generated in pineapple processing accounts for 50% of the total fruit weight (represented by crown, epicarp, and core) [21]. In the process of extracting oil from the sachá inchi seed, the byproduct represents 75% of the total seed weight [22]. These two wastes present high concentrations of carbohydrates and proteins, and therefore, they have great potential for use in bioprocesses [21, 22].

Agro-industrial wastes have been used in recent decades to formulate fermentation substrates [23, 24]. However, research into the use of agro-industrial residues continues to reduce metabolite production costs (20), produce probiotics and metabolites [25], produce polyunsaturated fatty acids under the concept of biorefineries [24], among other uses.

Micanquer-Carlosama et al. [25] formulated a fermentation substrate from pineapple and sachá inchi wastes, supplemented with mineral salts. This product showed promising results in the reproduction of the lactic acid bacterium *Weissella cibaria*. This substrate could be integrated as an aqueous phase in W/O emulsion formulations for subsequent applications (double emulsions, encapsulation of probiotics, controlled release of bioactive compounds, among others). At present, the scientific literature does not report investigations of the use of agroindustrial wastes in the formulation of emulsions. Therefore, this line of research would open

a path in the strengthening sustainable production systems, currently of great importance given the principles of circular economy [24, 26]. In this context, the research had two objectives: (i) to optimize the formulation and process of obtaining a W/O type emulsion using both a supplemented aqueous phase of pineapple and sachá inchi wastes combined with mineral salts and sunflower oil; and (ii) to evaluate their stability during short storage.

## 2. Methods

### 2.1. Materials

The core and peel of the pineapple variety "Oro Honey" were used at maturity stage 4 according to NTC 729-1 [27], from Valle del Cauca, Colombia. The by-product of the sachá inchi seed (cake obtained by extracting oil from the seed) from Putumayo, Colombia (supplied by Agroincolsa S.A.S.). Analytical grade salts from Sigma Aldrich, Germany were used:  $C_2H_3NaO_2$  (Sodium acetate) (purity 99.0%),  $C_6H_5O_7 \cdot 2NH_3$  (di-ammonium hydrogen citrate) (purity 98.0%),  $K_2HPO_4$  (dipotassium phosphate) (purity 98.8%),  $MgSO_4$  (Magnesium Sulfate) (purity 98%). Sunflower oil for its nutritional characteristics and its high content of monounsaturated fatty acids (oleic acid > 80%) and the surfactants Tween 80 (Oxiteno) (HLB 15) and Span 60 (Protécnica Ingeniería) (HLB 4.7) were used.

### 2.2. Formulation of W/O emulsions

The dispersed aqueous phase (W) was obtained according to the methodology described by Micanquer-Carlosama et al. [25]; it was formulated from a mixture of pineapple core and peel powder, the by-product of the sachá inchi and supplementation salts; the continuous phase (O) was sunflower oil. The emulsions were prepared by using a rotor-stator type homogenizer (Silverson Machines Ltd. Model L5M. England) with a standard emulsifier head that operated at 10000 rpm. Initially, the Tween 80 was diluted in the supplemented aqueous phase. The Span 60 was heated until it melted and then added to the oil phase. Finally, the aqueous phase was slowly added to the oil phase during the homogenization time (HT). For the development of the W/O emulsion, response surface methodology was used (central composite design,  $\alpha=1$ , 21 experiments). It considered four independent variables: HT (1 - 5 min),  $HLB_{total}$  (4.7 - 6.7), total surfactant (0.1 - 0.5%), and oil (30 - 50%); the dependent variables were: viscosity ( $\mu$ ), zeta potential ( $\zeta$ ), creaming index (CI), particle size (percentiles  $D_{10}$ ,  $D_{50}$ ,  $D_{90}$ , and  $D_{4,3}$ ), and the spectral absorbance stability index (R). The continuous phase content was calculated from the mass balance in batches of 200 g; the proportion of Tween 80 and Span 60 was determined from the  $HLB_{total}$  (Eq. 1). Where X and (1-X) are the mass fractions of Tween 80 and Span 60 [28].

$$HLB_{Total} = X HLB_{Tween\ 80} + (1-X) HLB_{Span60} \quad (1)$$

### Characterization of emulsions W/O

The  $\mu$  was determined by using a Brookfield DV-III Ultra Rotational Rheometer (Brookfield Engineering Laboratories, Inc., EE. UU), supplemented by ULA, with a velocity of 0.01-100 rpm, reporting at 100 rpm and 25°C [12]. The  $\zeta$  was determined by using the Zetasizer Nano ZS90 (Malvern Instruments Ltd., Worcester, UK) and following a modified methodology originally proposed by Li

et al. [1], where the findings were diluted (1:100) and the injection in the cell was 1 mL at 25°C. The software Standard Operating Procedure produced the results. The CI was determined by following a modified methodology originally described by Chang and McClements [8]; Muhamad et al. [4], 10 mL of the emulsion are transferred to 15 mL falcon tubes. Subsequently, the tubes were centrifuged at 1027 g for five minutes in a centrifuge (Hettich - Universal 320R, Germany). Finally, the relationship between the volume of the cream layer ( $V_C$ ) to the total volume of the emulsion ( $V_E$ ) determined the CI ( $CI(\%) = \frac{V_C}{V_E} * 100$ ).

The Mastersizer 3000 determined the particle size by using laser light diffraction (Malvern Instrument Ltd., Worcestershire, UK) and a Hydro LV system; sizes were expressed in the  $D_{10}$ ,  $D_{50}$ , and  $D_{90}$  percentiles including an equivalent volume diameter ( $D_{4,3}$ ) [8]; the refractive index of the supplemented aqueous phase (1.343 at 25°C) and the refractive index of water (1.33) were previously determined; the absorption index of the particle was set at 0.45 and the level of obscuration of the laser at 15 [29]. The R was determined with the absorbance relationship at 800 nm and 400 nm (A800/A400) [12] by using a UV-Visible spectrophotometer (Thermo Scientific Evolution 60, USA) and white like deionized water.

Finally, the microstructure of the W/O<sub>optimal</sub> emulsion was observed through micrographs obtained by an optical microscope (Leica ICC50 W, Switzerland) at 40× magnification.

### 2.3. Mathematic model and experimental optimization

The dependent variables described above were modeled as a function of the independent variables by means of a 2<sup>nd</sup> degree polynomial model (Eq. 2), where  $Y$  is the dependent variable,  $\beta_0$  is the model constant;  $\beta_A$ ,  $\beta_B$ ,  $\beta_C$ , and  $\beta_D$  are the linear coefficients;  $\beta_A^2$ ,  $\beta_B^2$ ,  $\beta_C^2$ , and  $\beta_D^2$  are the quadratic coefficients; and  $\beta_{AB}$ ,  $\beta_{AC}$ ,  $\beta_{AD}$ ,  $\beta_{BC}$ ,  $\beta_{BD}$ , and  $\beta_{CD}$  are the coefficients of the interactions between the independent variables ( $A$ ,  $B$ ,  $C$ , and  $D$ )

$$Y = \beta_0 + \beta_A A + \beta_B B + \beta_C C + \beta_D D + \beta_A^2 A^2 + \beta_B^2 B^2 + \beta_C^2 C^2 + \beta_D^2 D^2 + \beta_{AB} AB + \beta_{AC} AC + \beta_{AD} AD + \beta_{BC} BC + \beta_{BD} BD + \beta_{CD} CD \quad (2)$$

The data were analysed by using the ANOVA, with a significance level of 5% through the Statgraphics software, version 17.2.15. The experimental data of the dependent variables are reported as the mean value  $\pm$  standard deviation, obtained from measurements in triplicate for each experiment. The selection of the W/O emulsion was carried out by an experimental optimization from multiple responses, which guarantees the best physicochemical stability. Finally, validation of the optimised independent variables was performed by experimental runs in triplicate.

### 2.4. Storage

The physicochemical stability of the W/O<sub>optimal</sub> emulsion stored at 4°C, was evaluated from a unifactorial design; it considered both the storage time (1, 2, and 3 days) as the independent variable and  $\mu$ ,  $\zeta$ , CI,  $D_{10}$ ,  $D_{50}$ ,  $D_{90}$ ,  $D_{4,3}$ , and R as the dependent variables. A short storage time (0, 1, 2, 3 days) was considered because this simple emulsion is not a final product, it is an intermediate phase for the subsequent formulation of a double emulsion system, which will contain probiotic

microorganisms. (*W. cibaria*), where the final colloidal system will be induced to a process of encapsulation of the microorganism by complex coacervation.

### 3. Results and Discussion

#### 3.1. Self-assembly of the colloidal W/O system

The W/O emulsion was formed by homogenizing the aqueous phase (pineapple and sachá inchi wastes, and mineral salts) and the lipid phase (sunflower oil), in the presence of the emulsifiers Span 60 (HLB = 4.7) and Tween 80 (HLB = 15), capable of producing the W/O interface. For the formation of the emulsion, different phenomenologies associated with the forces involved in the stability or instability of the colloidal system under study converge. First, the structure of the assembly of the dispersed particles (aqueous phase) in the colloidal system starts from the supplied shear energy, which produces a large amount of small, dispersed particles with a high surface area and high free energy between the dispersed and continuous phases. This situation leads to a decrease in particle size. This ostensibly reduces the attractive forces or Van der Waals forces, which are responsible for colloidal instability. Second, the presence of the non-ionic surfactants used initially generates the formation of micellar groups that end up adsorbing at the particle interface due to their amphiphilic character (affinity of the functional groups present in both the dispersed and continuous phases). And third, the ions produced by dissociation of the salts present in the aqueous phase relocate in a layer attached to the interface with the electrical potential of opposite charge to the dispersed particles; whereas, the other ions, relocate in the electrical double layer, contributing to the strengthening of the repulsive forces between the particles and mainly responsible for the stability of the colloidal system.

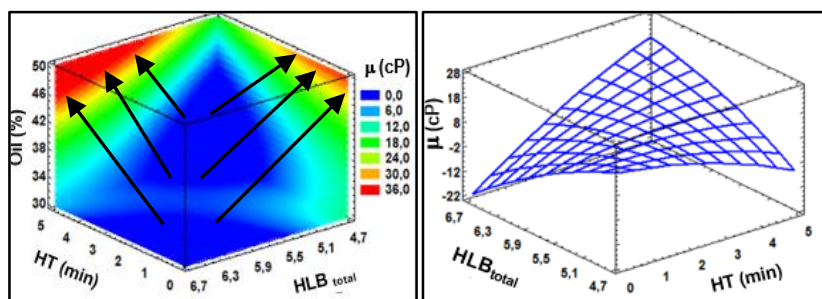
#### 3.2. Development of the W/O emulsion

Table 1 presents the mean values  $\pm$  standard deviation.

**Table 1. Results of the experimental design of the W/O emulsions based on the supplemented aqueous phase (pineapple and sachá inchi wastes, and mineral salts) and sunflower oil.**

RUN	Independent variables				Dependent variables							
	HT (min)	Surfactant (%)	HLB <sub>total</sub>	Oil (%)	$\mu$ (cP)	$\zeta$ (mV)	CI (%)	D <sub>10</sub> (μm)	D <sub>50</sub> (μm)	D <sub>90</sub> (μm)	D <sub>4,3</sub> (μm)	R
1	3	0.3	6.7	40	8.9±0.1	-49.6±1.2	8.3±0.1	1.1±0.0	4.7±0.3	150.4±4.8	41.3±2.1	0.962±0.016
2	5	0.3	5.7	40	12.9±1.4	-47.0±1.6	10.3±0.4	3.8±0.3	84.6±1.4	185.1±5.1	96.3±1.7	0.859±0.035
3	3	0.3	5.7	40	9.3±0.4	-46.1±0.7	43.3±0.0	1.5±0.0	28.4±0.2	93.2±1.3	40.4±1.7	0.985±0.014
4	1	0.5	4.7	30	13.4±2.1	-41.6±0.4	31.0±0.4	13.4±1.5	77.6±2.4	139.0±8.9	78.5±2.6	0.853±0.012
5	5	0.1	6.7	30	4.9±0.3	-43.6±1.3	41.3±0.1	20.3±0.7	58.7±0.6	144.8±4.9	214.1±2.2	0.919±0.013
6	3	0.3	5.7	30	3.7±0.2	-45.1±0.4	27.3±0.5	1.1±0.1	11.7±0.1	26.8±0.1	12.6±1.3	0.996±0.004
7	5	0.1	4.7	50	7.9±0.5	-47.0±1.0	51.7±0.2	16.8±0.3	54.6±0.3	127.0±5.6	66.6±1.4	0.961±0.011
8	5	0.5	4.7	50	20.8±1.6	-44.2±1.6	49.0±0.7	26.0±2.3	167.4±5.7	303.8±16.1	187.2±1.8	0.941±0.003
9	1	0.5	6.7	50	19.8±1.4	-46.7±0.3	55.7±0.2	1.2±0.0	26.4±0.1	107.6±1.2	40.8±1.1	0.908±0.001
10	3	0.5	5.7	40	12.2±0.7	-43.6±2.9	45.3±0.3	1.1±0.0	10.9±0.4	24.2±0.1	11.5±0.8	0.990±0.001
11	3	0.3	5.7	40	7.3±0.2	-44.2±1.5	35.7±0.1	1.2±0.0	17.2±0.1	36.1±0.5	17.8±1.0	0.967±0.005
12	1	0.3	5.7	40	7.2±0.5	-47.8±0.5	38.7±0.1	1.6±0.0	47.6±0.2	88.6±0.9	47.3±0.6	0.940±0.002
13	3	0.3	5.7	50	36.0±5.6	-43.8±1.9	18.3±0.3	41.5±2.3	154.0±9.6	291.6±13.2	189.0±2.0	0.833±0.013
14	3	0.3	4.7	40	8.2±0.2	-44.5±1.2	46.3±0.4	10.1±0.4	94.3±1.6	170.7±4.9	97.5±0.5	0.903±0.004
15	1	0.1	4.7	30	3.8±0.0	-43.7±1.7	29.7±0.2	36.4±1.3	138.0±6.2	262.8±13.8	159.2±1.0	0.827±0.02
16	3	0.3	5.7	40	7.4±0.5	-47.7±1.2	46.7±0.1	1.3±0.0	22.4±0.1	56.1±0.2	28.2±0.6	0.984±0.003
17	3	0.3	5.7	40	8.3±0.7	-49.8±2.1	39.7±0.2	1.5±0.0	29.5±0.1	51.0±0.2	28.6±0.4	0.974±0.003
18	5	0.5	6.7	30	4.8±0.9	-40.2±1.2	41.7±0.6	1.1±0.1	6.2±0.0	17.4±0.1	7.7±0.2	0.991±0.004
19	3	0.3	5.7	40	7.4±0.1	-45.1±1.6	51.0±0.2	1.2±0.0	14.2±0.0	28.8±0.1	14.4±0.5	0.985±0.002
20	1	0.1	6.7	50	7.2±0.4	-48.3±0.8	31.7±0.8	53.5±2.1	117.2±2.7	197.4±5.9	129.1±0.6	0.902±0.006
21	3	0.1	5.7	40	9.9±0.1	-48.6±1.5	36.7±1.0	54.8±3.7	131.6±4.5	237.6±9.3	153.1±0.9	0.917±0.014

Figure 1 presents the response surface graph and the main effects of  $\mu$  as a function of the independent variables. The  $\mu$  presented significant differences ( $p < 0.05$ ) concerning the oil content and the total surfactant in addition to the HT-HLB<sub>total</sub> interaction. The average values fluctuated between 3.7 and 36.0 cP. This categorizes the colloidal system as lightly viscous with significant mobility of its particles in the continuous phase, which favors interparticle interaction and possible colloidal instability if the collisions do not meet an energy minimum [30]. An increase in  $\mu$  is observed when increasing oil and surfactant content in the emulsion. This phenomenon can be attributed to the fact that the oil, despite being less dense than the aqueous phase, has a higher  $\mu$  [7, 31]. The effect of oil viscosity is reflected a greater extent when the emulsion is type W/O. In this case, this confers greater opposition of the fluid to tangential deformation. Additionally, with the increase of the oil content to the imposed homogenization conditions, the size of dispersed particles increases with a smaller interface area. The above means that a part of the micelles formed are absorbed in the interface of the particle with a higher concentration of surfactants due to its amphiphilic nature. Another part of the micelles remains dispersed in the continuous oily phase, causing the increase of  $\mu$  [32, 33].



**Fig. 1. Response volume and surface graph of and main effects of  $\mu$  in the W/O emulsions as a function of independent variables (HT, HLB<sub>total</sub>, total surfactant and oil).**

The hydrodynamic and colloidal interactions change the  $\mu$  of the colloidal system, increasing the degree of disturbance of the normal flow of liquid [2]. The extent to which a higher viscosity from the continuous phase is preserved, the greater the physicochemical stability of the emulsion, due to the lower mobility of the dispersed particles [5, 31]. On the other hand, the individual effect of HT was not influential with any dependent variable, which affected the HT-HLB<sub>total</sub> interaction positively. The trend of a high  $\mu$  is projected to high or low values of HT-HLB<sub>total</sub>; however, this would be consistent for low HLB<sub>total</sub> values where the higher lipophilic affinity of Span 60 would contribute to the  $\mu$  increase. This situation leads us to think that the amount of oil in the emulsion prevails over this HT- HLB<sub>total</sub> interaction. The rheological behavior obtained in the present study coincides with reports from Alliod et al. [31], who evaluated the effects of the composition and content of different mineral oils (continuous phase), reporting  $\mu$  values in the final emulsion between 4.3 and 17.8 cP. On the other hand, [34], report that the chemical composition of the oils influences the  $\mu$ , which is lower in vegetable oils (14.8 - 20.2 cP) due to the higher degree of unsaturation.

Figure 2 presents the  $\zeta$  response surface graph (A), where a trend of a greater  $|\zeta|$  (> (negative electric potential) is observed mainly at a lower content of surfactants. In effect, this could be simultaneously generating a decrease in the dielectric constant of the continuous medium and a modification of the electrical double layer thickness [19, 35]. Various authors have reported a strong criterion of physicochemical stability is when the  $|\zeta| > 30$  mV because the colloidal system has a predominance of repulsive electrostatic forces [5, 11, 18].

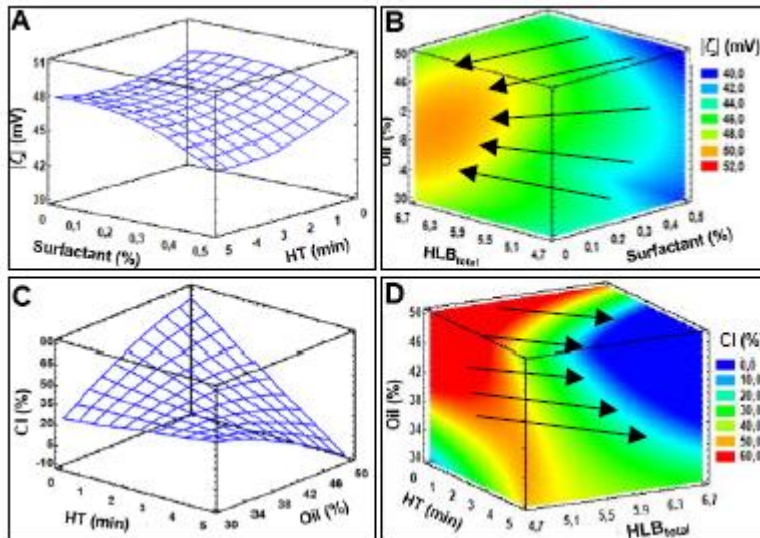


**Fig. 2. Response volume and surface graph of  $|\zeta|$  (A and B) and CI (%) (C and D) in W/O emulsions, as a function of the independent variables (HT, HLB<sub>total</sub>, total surfactant and oil)**

The  $\zeta$  represents the electric potential formed by the presence of positive and negative charges around the dispersed particle in a colloidal system. This property allows prediction of medium and long-term stability [18, 35, 36]. In the W/O emulsions, the  $\zeta$  presented statistically significant differences ( $p < 0.05$ ) concerning the total surfactant. The values fluctuated between -49.8 and -41.6 mV. These results indicate that to conditions of temperature and pH of  $24 \pm 1^\circ\text{C}$  and  $5.2 \pm 0.2$  respectively, the emulsions obtained have a high electric potential (-) in the adhered co-ions layer at the interface of the dispersed particles (Stern layer) [37]. Duffus et al. [38], showed that the pH and composition of emulsions significantly influence the  $\zeta$ , reporting higher negative electrical potentials (-55 mV) in acidic conditions and with a pH between 4.6 and 6.2. The co-ions layer is represented by anions mainly contributed by carboxylic groups dissociated to  $\text{COO}^-$  of the fatty acids present in the continuous phase (sunflower oil) and the internal surface charge of the aqueous particles is of the sign (+) because of the presence of dissociated cations from the supplemented aqueous phase salts (i.e.  $\text{C}_2\text{H}_3\text{NaO}_2$ ,  $\text{C}_6\text{H}_5\text{O}_7 \cdot 2\text{NH}_3$ ,  $\text{K}_2\text{HPO}_4$ , and  $\text{MgSO}_4$ ). Followed by the interface ion layer, a second diffuse layer is formed, mainly charged by ions contrary to those absorbed in the Stern layer (+). The charge density is greater with the increase of the double layer. In addition, when there is particle-particle interaction, it produces repulsive or electrostatic forces that are mainly

responsible for the observed colloidal stability [11, 15]. Results near and far have been replenished by Liu et al. [39], who reported the highest value of  $\zeta = -43.9$  mV. The authors evaluated double emulsions by using hydrogenated and unhydrogenated soybean oil in the oily phase. Similarly, Young et al. [40] obtained values between -37.1 and 87.7 mV in emulsions based on canola oil.

On the other hand, Fig. 2 (C and D) presents the CI response volume and surface graph as a function of the independent variables. A lower CI trend is mainly observed when the  $HLB_{total}$  was higher (6.3 - 6.7, blue zone). Even, the HT-Oil interaction favors the lowest CI at conditions of 38-48% and  $HT \approx 2-5$  min. This situation conditions the CI response to the characteristics of the W/O emulsion production and to the multivariate interaction of surfactants-Oil-HT, where a higher or lower CI on the surface is accompanied by aggregation at the bottom of aqueous particles [19]. However, the greatest effect presented by the total surfactant shows its emulsifying action against a centrifugal force when applied the accelerated stability [32]. Authors such as Vicente et al. [2], reported a decrease in stability during 14 days of storage ( $100 \rightarrow 11.0\%$ ) for emulsions based on sachu inchi oil; in contrast, Duffus et al. [38], reported greater instability in W/O type emulsions over O/W, observing phase separation at 24 h when using sunflower oil in the oily phase.

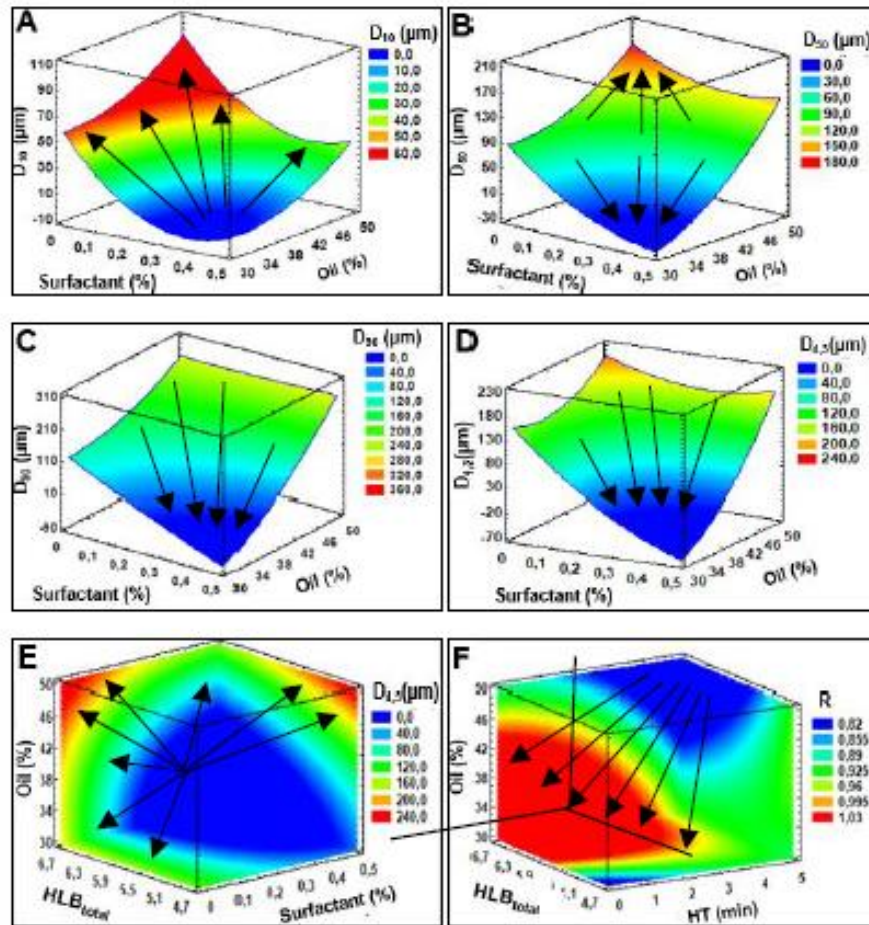
Creaming is a reversible process induced by gravity or by centrifugal action, which implies the formation of a vertical gradient of particle concentration without modifying its size distribution. This has been used as a reference to express the thermodynamic instability associated with droplet aggregation phenomena followed by a possible coalescence [9, 14]. The CI in the W/O emulsion presented statistically significant differences ( $p < 0.05$ ) concerning the  $HLB_{total}$  and the linear interaction HT-Oil. The average values fluctuated between 8.3 - 55.7%; this denotes an important difference in the volume of creaming induced by centrifugal action. Since, that action accelerates the rate of creaming formation (accelerated colloidal instability) when given the differences in densities between the continuous and dispersed phase [9]. The high CI values found could be favoured by the type of W/O emulsion, the composition of the phases, and the type of oil used. Since, the vegetable oils have low viscosity due to their rich composition in unsaturated fatty acids and because they can cream more easily than a more viscous oil [34].

Figure 3 presents the graphs of response surface for the  $D_{10}$ ,  $D_{50}$ ,  $D_{90}$ , and  $D_{4,3}$  (A, B, C, D) percentiles and the graphs response volume for  $D_{4,3}$  and R (E and F) in the W/O emulsions. W/O emulsions require surfactants with low  $HLB_{total}$  values; however, when studying colloidal systems under the evaluated conditions, the particle sizes obtained were not statistically affected.

In general, the three percentiles and  $D_{4,3}$  showed a similar behavior: a decreasing trend for  $D_{10}$ ,  $D_{50}$ , and  $D_{90}$  in formulations with lower oil content and higher surfactant content. This situation is attributed to the fact that the decrease in the oil content in the dispersed phase favors a higher ratio of the shear energy / mass of the dispersed phase, which produces a smaller particle size, a greater number of dispersed particles and a greater interfacial area. This increase in the interfacial area favors a greater absorption of the amphiphilic surfactants, to correct the high free energy between the continuous phase and the dispersed phase [19].



The  $D_{10}$  and  $D_{4,3}$  percentiles presented significant differences ( $p < 0.05$ ) concerning the oil and surfactant contents. Additionally,  $D_{4,3}$  presented a linear interaction whit  $HT-HLB_{total}$ , surfactant- $HLB_{total}$ , and surfactant- $HLB_{total}$ . On the other hand,  $D_{50}$  and  $D_{90}$  presented significant differences ( $p < 0.05$ ) only concerning oil content. The influence of these independent variables confers an important variation in the mean values of  $D_{10}$  (1.1 - 54.8  $\mu m$ ),  $D_{50}$  (4.7 - 164.7  $\mu m$ ),  $D_{90}$  (24.2 - 303.8  $\mu m$ ),  $D_{4,3}$  (7, 7 - 214.1  $\mu m$ ), and in the particle size distribution all at the same time. Particle size in colloidal systems is directly related to attractive forces, and these colloidal interactions can lead to physicochemical instability [15, 36]. Therefore, the surfactant action plays an important role due to the large accumulation of free energy at the interface given the lack of chemical affinity of the phases [5].



**Fig. 3. Response surface graph (A: $D_{10}$ ; B: $D_{50}$ ; C: $D_{90}$ ; D: $D_{4,3}$ ) and volume graph (E:  $D_{4,3}$ ; F: $R$ ) for particle size and  $R$  in W/O emulsions, as a function of the independent variables ( $HT$ ,  $HLB_{total}$ , total surfactant and oil).**

On the other hand, the presence of larger particle sizes generates a smaller surface area that adsorbs a smaller quantity of Tween 80 and Span 60 micelles.

However, at high concentrations of surfactants and mainly with high levels of oil, the Tween 80 micellar distribution at the interface could have a higher affinity, given the polarity of the dispersed particles. Even, a micellar excess of Span 60 remains in the continuous oily phase; without precipitating (no phase separation was observed). This could be increasing the  $D_{10}$ ,  $D_{50}$ , and  $D_{90}$  percentiles. Furthermore, the results of  $D_{4,3}$  are very consistent with the variability of sizes found in the  $D_{10}$ ,  $D_{50}$ , and  $D_{90}$ ; however, there is no well-defined trend in the behavior of  $D_{4,3}$  with its response being dependent on the combination of the independent variables.

Alliod et al. [31], reported in W/O emulsions, based on mineral oils (White, Fisher, and Marcol), that the droplet size was dependent on the  $\mu$  of the continuous phase, and reaching droplet sizes ( $D_{50}$ ) between 550 - 660 nm. Likewise, Okuro et al. [6], reported by using sunflower oil with W/O and O/W emulsions, drop sizes are between 2 - 4  $\mu\text{m}$  ( $D_{3,2}$ ). Additionally, the W/O emulsions showed an increase in the droplet size with the highest content of emulsifier (lecithin). Other investigations have reported small droplet sizes ( $D_{4,3}$ : 123.45 - 180.56 nm) in W/O emulsions based on vegetable oils (sunflower, olive, and red pepper), when subjected to a double homogenization process [41]. Young et al. [40], reported variability in droplet sizes ( $D_{50}$ ) (115.1 - 1132.9 nm) due to, the effect of applied treatments (heat treatment, high hydrostatic pressure).

The average values of  $R$  varied between 0.827 - 0.996, presenting significant differences ( $p < 0.05$ ) concerning the oil content and with the linear interactions HT- $HLB_{\text{total}}$  and Oil- $HLB_{\text{total}}$ . Because  $R$  is related to the scattering properties of light as it passes through the measurement cell. Greater light absorption is caused by the presence of a high density of smaller droplets, contributing to greater stability of the colloidal system [2, 12, 17]. The  $R$  values are considered high and consistent with the poly-dispersibility in the  $D_{10}$ ,  $D_{50}$ , and  $D_{90}$  percentiles. However, the emulsions were physio-chemically stable without showing phase separation, given the high synergy with the high negative electric potential in the vicinity of the particle interface ( $|\zeta| \gg \gg$ ). Similar results have been obtained in stable coconut-based colloidal systems (0.830-0.900) [3]; at the same time, other authors have reported lower values in stable colloidal systems based on avocado combined with certain spices ( $0.78 \pm 0.03$ ) [12], yacón ( $0.460 - 0.607$ ) [16], and the combination of egg and mango ( $0.679 \pm 0.002$ ) [42].

A trend for the decrease in  $R$  was observed with higher oil content, which corresponds to a lower content of the supplemented aqueous phase and greater action of shear energy on the size reduction. On the other hand, the linear interactions HT-  $HLB_{\text{total}}$  and Oil -  $HLB_{\text{total}}$  were negative, being more critical ( $>R$ ) to high  $HLB_{\text{total}}$  and low HT, as well as to high  $HLB_{\text{total}}$  and low oil content. This high  $HLB_{\text{total}}$  interaction could be due to the lower non-polar affinity that the total surfactant has under these conditions, which is empowered at low HT and oil contents, where the effect of homogenization generates larger particle sizes.

### 3.3. Mathematical modeling and experimental optimization of multiple responses

Table 2 presents the estimated regression coefficients of the 2<sup>nd</sup> order polynomial model for the W/O emulsion and their respective  $R^2$ . The  $R^2$  values for the dependent variables  $\mu$ ,  $\zeta$ ,  $D_{10}$ ,  $D_{50}$ ,  $D_{90}$ ,  $D_{4,3}$ , and  $R$  showed a good fit of the

mathematical model ( $R^2 > 80\%$ ); while the CI presented the lowest regression adjustment ( $R^2 = 71\%$ ); this is possibly due to the additional effect of the independent centrifugation operation, which could induce a greater error concerning the value predicted by the model. It is highlighted that all the variables presented a random distribution of the residuals, which makes it possible to ensure that the data can be parameterized according to a normal distribution; therefore, the models are adequate to describe the behavior of the results found.

**Table 2. Mathematical modeling of regression coefficients and  $R^2$  of the dependent variables ( $\mu$ ,  $\zeta$ , CI,  $D_{10}$ ,  $D_{50}$ ,  $D_{90}$ ,  $D_{4,3}$  y R) of the W/O emulsion.**

Regression coefficients	Dependent variables							
	$\mu$ (cP)	$\zeta$ (mV)	CI (%)	$D_{10}$ ( $\mu\text{m}$ )	$D_{50}$ ( $\mu\text{m}$ )	$D_{90}$ ( $\mu\text{m}$ )	$D_{4,3}$ ( $\mu\text{m}$ )	R
$\beta_0$	123.352	2.691	-492.07	235.581	1265.210	3836.680	1664.780	-2.000
$\beta_A$	-33.202	2.451	64.379	-37.346	-165.169	-401.688	-240.069	0.285
$\beta_B$	41.293	2.889	-278.25	-184.79	-164.974	-368.413	-155.881	-0.164
$\beta_C$	11.335	3.106	65.751	11.351	-129.367	-751.574	-229.173	0.536
$\beta_D$	-7.002	1.325	17.781	-9.797	-29.786	-59.349	-33.320	0.056
$\beta_A^2$	-0.544	0.152	-----	-1.934	2.397	2.323	1.931	-0.009
$\beta_{AB}$	-2.952	-0.771	-8.646	20.378	66.116	82.180	25.993	0.006
$\beta_{AC}$	6.271	-1.375	-5.021	8.457	30.259	55.457	46.343	-0.048
$\beta_{AD}$	0.076	0.112	-1.006	-0.121	-0.807	1.778	-0.781	0.001
$\beta_B^2$	-29.327	-18.15	299.023	437.603	368.484	83.593	455.552	0.412
$\beta_{BC}$	-6.329	-----	16.043	-36.152	-122.410	-168.889	-209.098	0.0450
$\beta_{BD}$	0.996	0.071	1.229	-0.059	8.437	21.139	19.957	-0.007
$\beta_C^2$	-3.699	0.224	-----	-4.819	-6.999	32.977	5.335	-0.005
$\beta_{CD}$	0.357	0.025	-1.862	0.615	2.758	6.245	1.599	-0.008
$\beta_D^2$	0.076	-0.024	-0.062	0.109	0.263	0.316	0.367	-0.001
$R^2$	92.573	82.414	71.156	89.566	86.105	80.279	91.545	88.076

Table 3 presents the criteria, weights, and impacts established in the experimental optimization of the W/O emulsion, the theoretical values predicted by the 2<sup>nd</sup> order model, the experimental values obtained from three replicas at the optimal condition, and the relative mean error (RME).

**Table 3. Criteria, weights, impacts and results of the experimental optimization of W/O emulsions.**

Dependent variables	Criteria	Weight	Impact	Theoretical Optimal	Experimental Optimal	RME (%)
R	Minimize	0.5	3	0.967	0.99±0.01	2.0
$\mu$ (cP)	19 cP	1.0	4	12.8	11.1±0.7	15.3
CI (%)	Minimize	1.0	4	23.9	22.3±0.5	7.2
$\zeta$ (mV)	-45 mV	0.5	3	-46.1	- 47.9±1.5	3.8
$D_{10}$ ( $\mu\text{m}$ )	Minimize	0.5	3	1.0	1.7±0.1	41.2
$D_{50}$ ( $\mu\text{m}$ )	Minimize	1.0	4	4.7	2.6±0.1	80.8
$D_{90}$ ( $\mu\text{m}$ )	Minimize	2.0	5	108.3	28.5±0.1	280
$D_{4,3}$ ( $\mu\text{m}$ )	Minimize	2.0	5	13.1	8.8±0.7	48.9

The experimental optimization of multiple responses presented the following results: HT = 3.73 min, surfactant = 0.47%,  $HLB_{\text{total}} = 6.53$ , and oil = 39.6%, with a desirability value of 70.1%, which corresponds to the best stability for the W/O emulsion. The experimental optimization validation of the dependent variables to the optimal conditions found presented lower values in  $D_{50}$ ,  $D_{90}$ , and  $D_{4,3}$  concerning the theoretical values, producing high values of the RME (41.2 -

80.8%). However, the point differences of these variables are not very noticeable (minimal), considering the poly-dispersibility observed in the particle sizes. The differences observed in the  $D_{90}$  percentile are much more notable, which is consistent with the greater variability found under the conditions of the experimental design (24.2 - 303.8  $\mu\text{m}$ ). Despite the point differences found, the experimental results of the validation of the optimum showed that the lower values of particle sizes contributed to better stability of the W/O emulsion [7].

Figure 4 presents a micrograph of the W/O emulsion at the optimal condition found. Spherical, well-defined, slightly flocculated droplets of varying sizes were observed. According to the results found, it is conferred that when considering the independent variables (HT, Surfactant,  $\text{HLB}_{\text{total}}$ , and oil) and their linear interactions, they do influence the morphology of the drops. This is because the size and particle size distribution are associated with the tension of the water-oil interface. At the same time, this depends on all the phenomena induced by the independent variables evaluated [10]. Drop size and similar morphology were reported by Chouaibi et al. (41), in a W/O emulsion based on olive and sunflower oil. On the other hand, Dai et al. [9], reported micrographs with homogeneous distribution and a size increase with a higher fraction of the short chain triglyceride oil used. However, other investigations identified differences in the distribution of the droplets formed in the W/O emulsions based on sunflower oil [6].

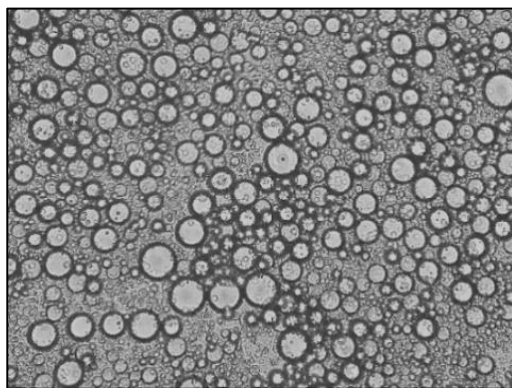


**Fig. 4. Micrographs of W/O<sub>optimal</sub> emulsion, obtained with an Optic Microscope (40X).**

### 3.4. W/O<sub>optimal</sub> emulsion stability during storage

Figure 5 illustrates the evolution of the dependent variables,  $\mu$ ,  $\zeta$ ,  $D_{10}$ ,  $D_{50}$ ,  $D_{90}$ ,  $D_{4,3}$ , and  $R$ , during the storage at 4°C for the W/O<sub>optimal</sub> emulsion. It was observed that the presented changes in the percentiles  $D_{10}$ ,  $D_{50}$ ,  $D_{90}$ ,  $D_{4,3}$ , and  $R$  were not significant. However, the rheological behavior of the emulsion shows a slight increase in  $\mu$  over time. This could infer that various physicochemical phenomena are being promoted due to: 1) increased energy in the interfacial region of the emulsion, which could confer a structural reorganization in the particle size distribution and the possible formation of flocs over time [43]; 2) reorganization of the size of the Span 60 micelles that could be in excess in the oil phase [10], and; 3) the reorganization of the Tween 80 micelles that could be located in the hydrophilic part of the same micelles [13].

According to the behavior and appearance observed in the emulsions, a good stability of the same emulsions is admitted during the 3 days of storage. This is mainly because the important levels of the electrical potential in the Stern layer are maintained ( $-47,9 \pm 1,5$  and  $-41,4 \pm 1,9$  mV). Likewise, the stability of the emulsion through repulsive forces is guaranteed within the diffuse layer of the particles, configuring a wide electrical double layer [15].

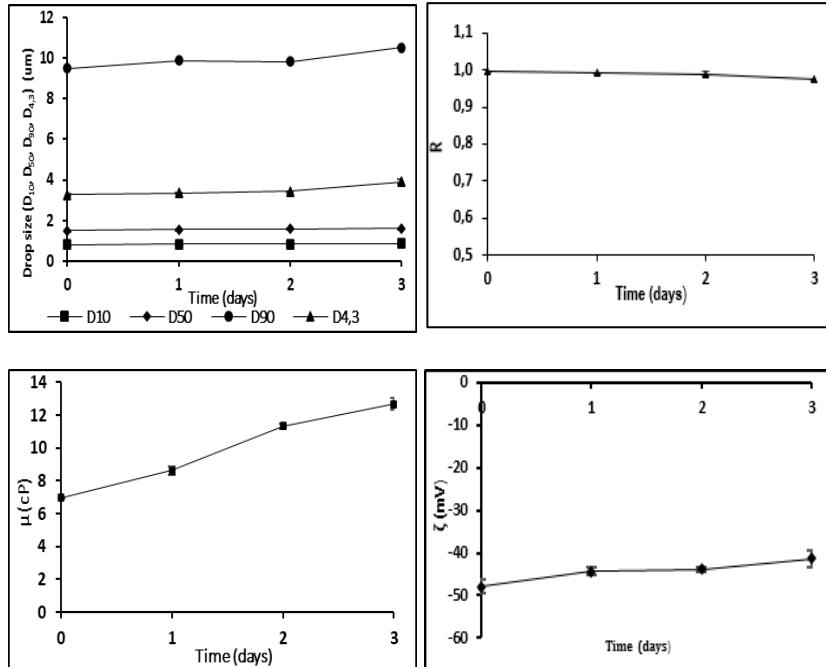


**Fig. 5. Stability of the dependent variables ( $\mu$ ,  $\zeta$ ,  $CI$ ,  $D_{10}$ ,  $D_{50}$ ,  $D_{90}$ ,  $D_{4,3}$  y  $R$ ) of the  $W/O_{\text{optimal}}$  emulsion during storage.**

#### 4. Conclusions

A W/O emulsion composed of a continuous phase based on sunflower oil and a dispersed aqueous phase formulated from agro-industrial wastes of pineapple, sachá inchi, and supplements (sources of macro and micronutrients) was formulated under optimized process and formulation conditions. The emulsion was characterized by low viscosity and excellent physicochemical stability. This was due to the predominance of the repulsive forces generated by the double electrical layer formed at the interface of the colloidal system particles, which were stronger than the attraction forces caused by small, spherical, homogeneous, and little flocculated drops. The  $W/O_{\text{optimal}}$  emulsion practically conserved its properties during three days of storage:  $\mu = 12.67 \pm 0.36$  cP,  $\zeta = -41.40 \pm 1.90$  mV,  $D_{10} = 0.84 \pm 0.01$   $\mu\text{m}$ ,  $D_{50} = 1.59 \pm 0.01$   $\mu\text{m}$ ,  $D_{90} = 10.54 \pm 0.04$   $\mu\text{m}$ ,  $D_{4,3} = 3.91 \pm 0.09$   $\mu\text{m}$ , and  $R = 0.97 \pm 0.01$ . The developed emulsion provides potential alternatives for further applications in double emulsions, encapsulation of probiotics, controlled release of bioactive compounds, among others, strengthening sustainable production systems.

## Acknowledgements

The authors thank to Ministry of Science, Technology, and Innovation of Colombia (Minciencias) for financing this research project.

### Nomenclatures

1-X	Span 60 mass fraction in the mix
$A_{400}$	Absorbance 400 nm
$A_{800}$	Absorbance 800 nm
$C_I$	Creaming index
$D_{10}$	Percentile 10%
$D_{4,3}$	Equivalent volume diameter
$D_{50}$	Percentile 50%
$D_{90}$	Percentile 90%
Emulsion W/O	Water in oil emulsion
$HLB_{total}$	Total Hydrophile-Lipophile Balance
HT	Homogenization time
R	Spectral absorption index
RME	Relative mean error
$V_C$	Cream layer volume
$V_E$	Emulsion total volume
$V_E$	Total volume of the emulsion
W/O/W - O/W/O	Double emulsion
X	Tween 80 mass fraction in the mix

### Greek Symbols

$\zeta$	Zeta potential
$\mu$	Viscosity

## References

- Li, B.; Jiang, Y.; Liu, F.; Chai, Z.; Li, Y.; Li, Y.; and Leng, X. (2012). Synergistic effects of whey protein-polysaccharide complexes on the controlled release of lipid-soluble and water-soluble vitamins in W1/O/W2 double emulsion systems. *International journal of food science & technology*, 47(2), 248-54.
- Vicente, J.; Barreto, L.J.; Heckert, L.P.; De Carvalho, M.G.; and Garcia, E.E. (2018). Effect of xanthan gum or pectin addition on Sacha Inchi oil-in-water emulsions stabilized by ovalbumin or tween 80: Droplet size distribution, rheological behavior and stability. *International journal of Biological Macromolecules*, 120, 339-45.
- Lucas, J.C.; Tobón, C.; and Cortés, M. (2018). Influence of the composition of coconut-based emulsions on the stability of the colloidal system. *Advances Journal Food Science Technology*, 14(3), 77-92.
- Muhamad, II.; Quin, C.H.; and Selvakumaran, S. (2016). Preparation and evaluation of water-in-soybean oil-in-water emulsions by repeated premix membrane emulsification method using cellulose acetate membrane. *Journal Food Science Technology*, 53(4), 1845-55.
- Tadros, T.F. (2016). *Emulsions: Formation, stability, industrial applications*. In: Walter de Gruyter GmbH & Co KG. p, 1-220.
- Okuro, P.K.; Gomes, A.; Costa, A.L.; Adame, M.A.; and Cunha, R.L. (2019). Formation and stability of W/O-high internal phase emulsions (HIPEs) and derived O/W emulsions stabilized by PGPR and lecithin. *Food Research International*, 122(2), 252-62.

7. Lei, J.; Gao, Y.; Ma, Y.; Zhao, K.; and Du, F. (2019). Improving the emulsion stability by regulation of dilational rheology properties. *Colloids and Surfaces A: Physicochemical and Engineering Aspects*, 583(3),123906.
8. Chang, Y.; and McClements, D.J. (2015). Interfacial deposition of an anionic polysaccharide (fucoidan) on protein-coated lipid droplets: Impact on the stability of fish oil-in-water emulsions. *Food Hydrocolloid*, 51, 252-60.
9. Dai, L.; Sun, C.; Wei, Y.; Mao, L.; and Gao, Y. (2018). Characterization of Pickering emulsion gels stabilized by zein/gum arabic complex colloidal nanoparticles. *Food Hydrocolloid*, 74, 239-48.
10. Nesterenko, A.; Drelich, A.; Lu, H.; Clausse, D.; and Pezron, I. (2014). Influence of a mixed particle/surfactant emulsifier system on water-in-oil emulsion stability. *Colloids and Surfaces A: Physicochemical and Engineering Aspects*, 457(1), 49-57.
11. Doğan, M.; Göksel, M.; and Aslan, D. (2020). Effect of salt on the inter-relationship between the morphological, emulsifying and interfacial rheological properties of O/W emulsions at oil/water interface. *Journal of Food Engineering*, 275 (4)2, 109871.
12. Estrada, E.M.; Rodríguez, M.C.; and Correa, G.A. (2017). Stability of a colloidal system based on avocado (*Persea americana* Mill.cv. Hass)and others: Effect of process and composition. *Agroindustry Food Science*, 66(3), 338-46.
13. Zhao, S.; Tian, G.; Zhao, C.; Li, C., Bao, Y., DiMarco-Crook, C.; Tang, .Z; Li, C.; McClements, D.; Xiao, H.; and Zheng, J. (2018). The stability of three different citrus oil-in-water emulsions fabricated by spontaneous emulsification. *Food Chemistry*, 269, 577-87.
14. McClements, DJ. (2015). *Food emulsions: Principles, practices, and techniques*. CRC press, 1-26.
15. Feng, Y.; Kilker, S.R.; and Lee, Y. (2020). *Surface charge (zeta-potential) of nanoencapsulated food ingredients*. Chapter Seven - In: Jafari SMBT-C of NFI, editor. *Characterization of nanoencapsulated food ingredients*. Academic Press, 213-41.
16. Arango, M.I.; Cortés, M.; and Largo, E. (2019). Stability of a colloidal suspension of yacon (*Smallanthus sonchifolius*) intended for spray drying. *Revista Facultad Nacional Agronomía*, 72(2), 8863-71.
17. Homayoonfal, M.; Khodaiyan, F.; and Mousavi, M. (2015). Modelling and optimising of physicochemical features of walnut-oil beverage emulsions by implementation of response surface methodology: Effect of preparation conditions on emulsion stability. *Food Chemistry*, 174, 649-59.
18. Ravindran, S.; Williams, M.A.; Ward, R.L.; and Gillies, G. (2018). Understanding how the properties of whey protein stabilized emulsions depend on pH, ionic strength and calcium concentration, by mapping environmental conditions to zeta potential. *Food Hydrocolloid*, 79, 572-8.
19. Hong, I.K.; Kim, S.I.; and Lee, S.B. (2018). Effects of HLB value on oil-in-water emulsions: Droplet size, rheological behavior, zeta-potential, and creaming index. *Journal of Industrial and Engineering Chemistry*, 67, 123-31.
20. Carpinelli, J.V.; De Barros, F.F.; Escaramboni, B.; Campioni, T.S.; Fernández, E.G.; and De Oliva, P. (2020). Cost-effective lactic acid production by fermentation of agro-industrial residues. *Biocatalysis and Agricultural Biotechnology*, 27, 101706.
21. Sepúlveda, L.; Romani, A.; Aguilar, C.N.; and Teixeira, J. (2018). Valorization of pineapple waste for the extraction of bioactive compounds and glycosides using autohydrolysis. *Innovative Food Science & Emerging Technologies*, 47, 38-45.
22. Wang, S.; Zhu, F.; and Kakuda, Y. (2018). Sacha inchi (*Plukenetia volubilis* L.): Nutritional composition, biological activity, and uses. *Food Chemistry*, 265, 316-28.

23. Sepúlveda, L.; Laredo, E.; Buenrostro, J.J.; Ascacio, J.A.; Genisheva, Z.; Aguilar, C.; and Teixeira, J. (2020). Ellagic acid production using polyphenols from orange peel waste by submerged fermentation. *Electronic Journal of Biotechnology*, 43, 1-7.
24. Greses, S.; Tomás, E., and González, C. (2020). Agroindustrial waste as a resource for volatile fatty acids production via anaerobic fermentation. *Bioresource technology*, 297, 122486.
25. Micanquer, A.; Cortés, M.; and Serna, L. (2020). Formulation of a fermentation substrate from pineapple and sacha inchi wastes to grow *Weissella cibaria*. *Heliyon*. 6(4), e03790.
26. Dahiya, S.; Kumar, A.N.; Shanthi, J.; Chatterjee, S.; Sarkar, O.; and Mohan, S.V. (2018). Food waste biorefinery: Sustainable strategy for circular bioeconomy. *Bioresource Technology*, 248, 2-12.
27. ICONTEC. (1996). Norma Técnica Colombiana. NTC 729-1. Frutas frescas. Piña, especificaciones. 1-13.
28. Nejadmansouri, M.; Hosseini, M.H.; Niakosari, M.; Yousefi, G.H.; and Golmakani, M.T. (2016). Physicochemical properties and oxidative stability of fish oil nanoemulsions as affected by hydrophilic lipophilic balance, surfactant to oil ratio and storage temperature. *Colloids and Surfaces A: Physicochemical and Engineering Aspects*, 506, 821-32.
29. Linke, A.; Hinrichs, J.; and Kohlus, R. (2020). Impact of the powder particle size on the oxidative stability of microencapsulated oil. *Powder Technology*, 364, 115-122.
30. Zheng, L.; Cao, C.; Chen, Z.; Cao, L.; Huang, Q.; and Song, B. (2020). Evaluation of emulsion stability by monitoring the interaction between droplets. *LWT - Food Science Technology*, 132, 109804.
31. Alliod, O.; Messenger, L.; Fessi, H.; Dupin, D.; and Charcosset, C. (2019). Influence of viscosity for oil-in-water and water-in-oil nanoemulsions production by SPG premix membrane emulsification. *Chemical Engineering Research and Design*, 142, 87-99.
32. Tripathy, D.B.; Mishra, A.; Clark, J.; and Farmer, T. (2018). Synthesis, chemistry, physicochemical properties and industrial applications of amino acid surfactants: A review. *Comptes Rendus Chimie*, 21(2), 112-30.
33. Wang, Y.; Hartel, R.W.; and Zhang, L. (2021). The stability of aerated emulsions: Effects of emulsifier synergy on partial coalescence and crystallization of milk fat. *Journal of Food Engineering*, 291, 110257.
34. Abdul, M.; Adewale, S.; Abdulwahab, I.; and Olakunle, A. (2020). Viscosity-temperature stability, chemical characterization, and fatty acid profiles of some brands of refined vegetable oil. *Physical Chemistry Research*, 8(3), 417-27.
35. Wu, Z.; Wu, J.; Zhang, R.; Yuan, S.; Lu, Q.; and Yu, Y. (2018). Colloid properties of hydrophobic modified alginate: Surface tension,  $\zeta$ -potential, viscosity and emulsification. *Carbohydrate polymers*, 181, 56-62.
36. Dukhin, A.S.; and Xu, R. (2020). Zeta-potential measurements. In: *Hodoroaba V-D, Unger WES, Shard AGBT-C of N. Chapter 3.2.5. Characterization of Nanoparticles*, 213-24.
37. Ondo, D. (2020). Thermodynamic study on complexation of long-chain fatty acid anions with  $\alpha$ -cyclodextrin in water. *Journal of Molecular Liquids*, 311, 113172.
38. Duffus, L.J.; Norton, J.E.; Smith, P.; Norton, I.T.; and Spyropoulos, F. (2016). A comparative study on the capacity of a range of food-grade particles to form stable O/W and W/O Pickering emulsions. *Journal Colloid Interface Science*, 473, 9-21.
39. Liu, J.; Kharat, M.; Tan, Y.; Zhou, H.; Muriel, J.L.; and McClements, D.J. (2020). Impact of fat crystallization on the resistance of W/O/W emulsions to osmotic stress: Potential for temperature-triggered release. *Food Research International*, 134, 109273.



40. Young, S.; Basiana, E.; and Nitin, N. (2018). Effects of interfacial composition on the stability of emulsion and encapsulated bioactives after thermal and high pressure processing. *Journal of Food Engineering*, 231, 22-9.
41. Chouaibi, M.; Mejri, J.; Rezig, L.; Abdelli, K.; and Hamdi, S. (2019). Experimental study of quercetin microencapsulation using water-in-oil-in-water (W1/O/W2) double emulsion. *Journal of Molecular Liquids*, 273, 183-91.
42. Ramirez, L.M.; Rodriguez, M.; Agudelo, Y.; and Ortega, R. (2020). Influence of atomization process and formulation on the development an egg and mango based powder food complement. *SYLGUAN*, 164, 493-514.
43. Velderrain-Rodríguez, G.R.; Acevedo-Fani, A.; González-Aguilar, G.A.; and Martín-Belloso, O. (2019). Encapsulation and stability of a phenolic-rich extract from mango peel within water-in-oil-in-water emulsions. *Journal of Functional Foods*, 56, 65-73.